Ex situ mineral carbonation for CO_2 mitigation: Evaluation of mining waste resources, aqueous carbonation processability and life cycle assessment (Carmex project)

F. Bodénan [a,*], F. Bourgeois [b], C. Petiot [c], T. Augé [a], B. Bonfils [b], C. Julcour-Lebigue [b], F. Guyot [d], A. Boukary [c], J. Tremosa [a], A. Lassin [a], E.C. Gaucher [e], P. Chiquet [e]

[a] *BRGM, 3 Avenue C. Guillemin, BP 36009, 45060 Orléans Cedex 2, France*
[b] *Université de Toulouse, Laboratoire de Génie Chimique (LGC), Toulouse, France*
[c] *Bio-IS, Paris, France*
[d] *IPGP, Paris, France*
[e] *CSTJF, TOTAL, Pau, France*

Keywords:
Carbonation
Mafic/ultramafic rocks
Slag
Mechanical exfoliation
Mineralogy

A B S T R A C T

This article presents the main outputs from the multidisciplinary Carmex project (2009–2012), which was concerned with the possibility of applying ex situ mineral carbonation concepts to mafic/ultramafic mining wastes. Focus points of the project included (i) matching significant and accessible mining wastes to large CO_2 emitters through a dedicated geographical information system (GIS), (ii) analysis of aqueous carbonation mechanisms of mining waste and process development and (iii) environmental assessment of ex situ mining waste carbonation through life cycle assessment (LCA) methodology. With a number of materials associated with the mining sector, the project took a close look at the aqueous carbonation mechanisms for these materials and obtained unexpected carbonation levels (up to 80%) by coupling mechanical exfoliation and reactive carbonation. Results from this work support the possibility of processing serpentine-rich peridotites without applying the classical first step of heat activation. Perspectives are also given for the carbonation of Ni-pyrometallurgical slag available closed to ultramafic mining residues. LCA of the mining waste carbonation system as a whole made it clear that the viability of this CO_2 storage option lies with the carbonation process itself and optimisation of its operating conditions. By combining the body of knowledge acquired by this project, it is concluded that New Caledonia, with its insularity and local abundance of 'carbonable' rocks and industrial wastes coupled with significant greenhouse gas (GHG) emissions from world-class nickel pyro and hydrometallurgical industries stands out as a strong potential candidate for application of ex situ mineral carbonation.

1. Introduction

Mineral carbonation is a natural weathering process that has led, albeit on a geological timeframe, to the formation of the carbonate rocks that constitute the main carbon reservoirs on Earth. Carbon dioxide Capture and Storage by Mineral carbonation (CCSM) include all the technologies developed to store CO_2 emissions as stable inert solid carbonates. The feedstock to such processes include rocks with high-bearing magnesium (Mg), calcium (Ca) and iron (Fe(II)) silicates, and some industrial residues. CCSM is described (IPCC, 2005; Sanna et al., 2012) as a possible alternative solution to geological CO_2 storage, the leading option for storing industrial CO_2 emissions on a global scale. The use of this natural exothermic process to capture industrial CO_2 emissions was proposed by Seifritz (1990) some twenty years ago, and numerous protocols have been developed since: reviews published by Huijgen and Comans (2003, 2004), Sipilä et al. (2008) and Doucet (2011) provide a comprehensive account of the technical solutions studied to date. Among them, direct aqueous carbonation stands as one of the most realistic options for large scale implementation. Acceleration of natural processes is typically implemented at high temperature and pressure (150–180 °C and 150 bars, O'Connor et al., 2001, 2004), preferably in an aqueous medium, with or without additives. Additives can be either inorganic (Gerdemann et al., 2007) or organic (Olsen and Rimstidt, 2008; Krevor and Lackner, 2011; Bonfils et al., 2012). The efficiency of the process being surface dependent, a fine grinding step of the rocks is invariably applied prior to the carbonation reaction. Typically, the rocks are ground below 50–200 μm, and sometimes as

* Corresponding author. Tel.: +33 (0)2 38 64 34 41; fax: +33 (0)2 38 64 30 62.
E-mail address: f.bodenan@brgm.fr (F. Bodénan).

http://dx.doi.org/10.1016/j.mineng.2014.01.011

fine as 4 μm (O'Connor et al., 2001; Gerdemann et al., 2007; Garcia et al., 2010). Heat activation of serpentine-type rocks (McKelvy et al., 2004; Gerdemann et al., 2007; Alizadehhesari et al., 2012) is also needed to increase reaction rate; this pre-treatment allows serpentine conversion into olivine above 550–650 °C, by the removal of physisorbed water and, then partial or complete dehydroxylation depending on temperature.

The buildup of a passivating layer around reacting particles is inevitable under aqueous carbonation of silicates. This is a true bottleneck for development of a viable process (Stockmann et al., 2011; Guyot et al., 2011). Being able to limit the formation of passivation layers, understanding and modelling the conditions leading to the formation of high porosity permeable layers and search for sub-products applications are key points that still need intense research.

From a water–rock interaction point of view, aqueous mineral carbonation is described by two distinct reactions (Chen et al., 2006): first the 'carbonable' cations Mg^{2+} (Ca^{2+}, Fe^{2+}) are leached out of the material, and then they react with dissolved CO_2 ($HCO3^-$) to form solid carbonates. The overall exothermic dissolution-precipitation reaction is typically written for forsterite as:

$$Mg_2SiO_4 + CO_2 + 2H_2O \rightarrow 2MgCO_3 + H_4SiO_4.$$

Depending on the conditions, serpentinization-like reaction can also occur:

$$2Mg_2SiO_4 + CO_2 + 2H_2O \rightarrow Mg_3Si_2O_5(OH)_4 + MgCO_3.$$

Typical rocks suitable for carbonation are ultramafic rocks (i.e. peridotite, amphibolite, pyroxenite, serpentinite) and mafic rocks (i.e. basalt, gabbro). They are also sometimes described as ultrabasic and basic rocks, depending on their SiO_2 content, which is <45% and 45–52% respectively (Foucault and Raoult, 2005). Also industrial residues described as alkaline high temperature process residues such as steel slag (Huijgen et al., 2005) or various types of combustion ash (Renforth et al., 2011), containing lime or cement-type mineral phases can be good candidate for carbonation.

Up to date aqueous mineral carbonation gave the most promising results; research on energy and cost efficient process development, possibly with pilot scale demonstrators is still needed. This way, this still non-economic viable route could become a longer term option through also a comprehensive study of potential applications of the carbonation products (Sanna et al., 2012).

This article presents the main outputs from a multidisciplinary project (2009–2012) co-funded by the French Agency Research (ANR), which was concerned with the possibility of applying ex situ mineral carbonation concepts to mining wastes. Focus points of the project included (i) matching significant and accessible mining wastes to large CO_2 emitters through a dedicated geographical information system (GIS), (ii) analysis of aqueous carbonation mechanisms of mining waste and process development and (iii) environmental assessment of ex situ mining waste carbonation through life cycle assessment (LCA) methodology.

The project focus was directed towards mine tailings that bear significant quantities of mafic and ultramafic rocks. Being already excavated and crushed, mine tailings carry obvious economic and environmental incentives for use as feedstock to the aqueous mineral carbonation process. In other words, mine tailings can be tagged as early opportunities for the development of CCSM.

2. Worldwide potential for ex situ mineral carbonation

2.1. A dedicated geographical information system (GIS)

World data on (i) CO_2-emission sites (IEA, 2006) and (ii) mining activities associated with ore deposits in mafic/ultramafic (M/UM) contexts (Rundqvist et al., 2006) have been cross-examined through a GIS (under ArcGIS) in order to identify large and super-large mining sites of potential interest for implementing the ex situ carbonation method on a worldwide scale (Picot et al., 2011). To reduce mining, grinding and transportation costs it was deemed essential to focus on currently operating or future planned mining sites, as discussed recently also by Hitch et al., 2009 and Hitch and Dipple (2012).

Fig. 1 shows that large CO_2 emission sites within 300 km, which is the maximum distance to avoid CO_2 recompression stages with pipelines, of one or several associated large UM rocks deposits are very unevenly distributed. This is related to the fact that certain regions of the globe, such as North America, Europe, India, China and Japan where CO_2 emissions sites are very numerous, are relatively devoid of (very) large UM deposits. Combining criteria about the nature and quantity of mining wastes, volumes of CO_2 emissions, distance between mine and emission sites, has pinpointed eight 'super large' potential ore deposits in an UM context, all within a 300 km radius of coal-fired industrial plants emitting over 1 Mt/year CO_2 (Picot et al., 2011).[1] Coal-fired power plants were first considered because of the higher concentrated CO_2 fluxes compared to other industries and UM resources as the richest in carbonable ions.

2.2. An example of prioritization

An attempt was then made to rank the eight sites, taking geographical and political considerations into account. Results are presented in Table 1. They embed the potential mining value of the residues – namely those containing diamond –, country accessibility and the total length of pipelines to transport the CO_2 from the emission sites, taking into account local topography as a key technical parameter. For this an average slope has been calculated using the GTOPO30 global digital elevation model of USGS.

The criteria used above are stringent, which explains the very small number of sites identified as early opportunities for ex situ mineral carbonation. This example was intended as a demonstration of the value of using GIS-based technology for decision-making about implementation of mineral carbonation around the globe. Indeed, other less severe criteria could be used using the same GIS tool and methodology, which would yield different potential sites, for example using shorter transport distances, using UM and also M resources, etc. It could also be further improved by adding hydrographical, chemical, mineralogical and economic criteria. The outcomes of this analysis can be compared locally with the corresponding geological storage potential evaluation.

2.3. Prospects in New Caledonia

Smaller sites with important local stakes in Europe, America, but also island contexts should be considered as possible opportunities for application of CCSM. Namely, the project considered New Caledonia as a prime candidate for the deployment of CCSM in the New Caledonian nickel mining context, given: (i) Its insularity i.e. with resources relatively close to CO_2 emissions, (ii) the abundance of accessible rocks and also industrial waste presenting real carbonation potential. Note that geological storage in fractured peridotites representing about 40% on the surface of the island could be an alternative source of carbonable material but mechanisms and processes are at the moment largely unknown and should be studied in parallel as part of portfolio solutions considering the extensiveness of the industrial CO_2 emissions derived from

[1] Data are accessible through kml files using Google Earth software at http://carmex.brgm.fr/.

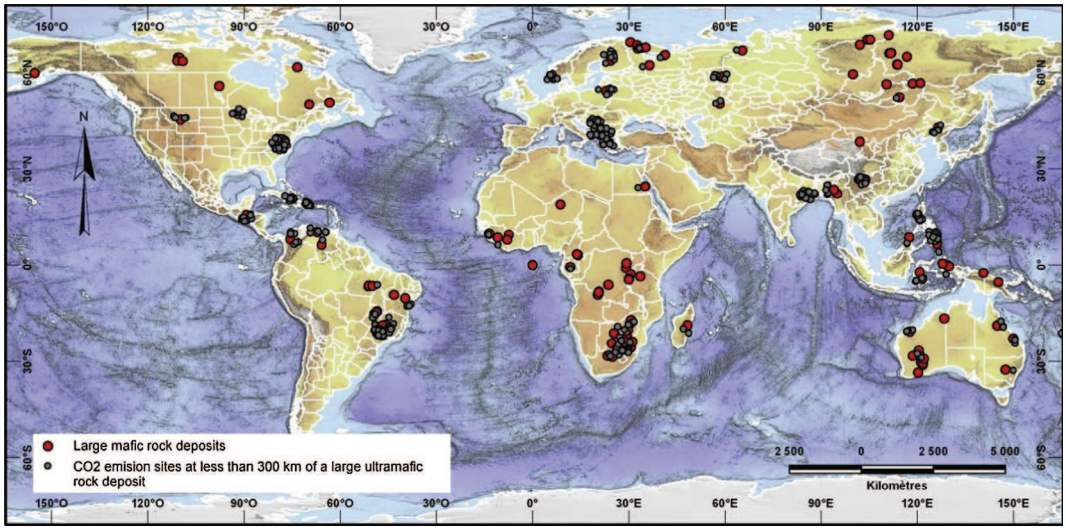

Fig. 1. Ore deposits related to ultramafic rocks lying less than 300 km from a CO_2-emission site.

Table 1
Example of worldwide superlarge sites potentially available for ex situ mineral carbonation with an attempt of prioritization.

Superlarge (class 4) UM ore deposits			Parameters				CO2 emission sites within 300 km			
Name	Country	Main commodity	Estimated volume of waste	Accessibility	Distances (km)	Average slope	CO_2 sites nb	Country	Total CO_2 kt/y	Main fuel
Phalaborwa	Sth Africa	Cr_2O_3	> 1 Gt	Good	78 - 271	2.9 - 8.3	2	Sth Africa	11 571	Coal
Bushveld Nth	Sth Africa	Cr_2O_3	> 1 Gt	Good	119 - 295	3 - 11.1	6 1	Sth Africa Botswana	80 748	Coal
Premier	Sth Africa	diamond	> 1 Gt	Difficult	98 - 256	3 - 6.6	1 4	Sth Africa	149 033	Coal
Orapa	Botswana	diamond	~ 350 Mt	Difficult	230 - 262	0.1 - 0.5	1 2	Botswana Zimbabwe	7 865	Coal
Jwaneng	Botswana	diamond	~ 250 Mt	Difficult	211 - 267	1.7 - 2.0	2	Sth Africa	7 547	Coal
Panzhihua	China	Fe	> 100 Mt	Very difficult	96 - 249	12 - 13.5	6 1	China India	47 404	Coal
Kempirsai	Kazakhstan	Cr_2O_3	>100 Mt	Very difficult	111	0.8	1	Russia	1 179	Coal
Kachkanarskoye	Russia	Fe, V_2O_5, TiO_2, PGE	> 10 Gt	Very difficult	101 - 178	2 - 3.7	1	Russia	15 445	Coal

existing and planned pyro- and hydrometallurgical processing of nickel ore. Figures are unknown at this stage but are in relation with the power of the coal power plants dedicated to these mining operations: 370 MW (in construction) and 165 MW (planned).

3. Materials and methods

3.1. Materials

As stated above typical rocks that can be carbonated are ultramafic (UM) rocks (i.e. peridotite, amphibolite, pyroxenite, serpentinite) and mafic (M) rocks (i.e. basalt, gabbro). Ferromagnesian minerals (olivine, orthopyroxene, serpentine) and calcium-bearing minerals (clinopyroxene, plagioclase, amphibole), which represent 90% of UM rocks, are the best candidates for mineral carbonation on a large scale.

Three types of material associated with the mining sector were tested in the project: natural peridotites (harzburgite – Hz1 and Hz2 – and wehrlite We1) collected in New Caledonia and lherzolite Lz1 from the type locality (French Pyrenees). The proportion of each initial mineral – i.e. without considering serpentinisation – in the three rock types is given in Fig. 2. The rocks have typical composition of rocks from the Earth's mantle i.e. largely present all over the world. Slag from SLN Doniambo nickel pyrometallurgy plant in Nouméa, New Caledonia, was also sampled (Fig. 3); they correspond to hot slag quenched into millimetric particles by spraying sea water on the pouring slag at the electric oven outlet. Slags are greenish[2] with brownish particles in relation with the presence of two main mineral phases observed by binocular

[2] For interpretation of colour in Fig. 3, the reader is referred to the web version of this article.

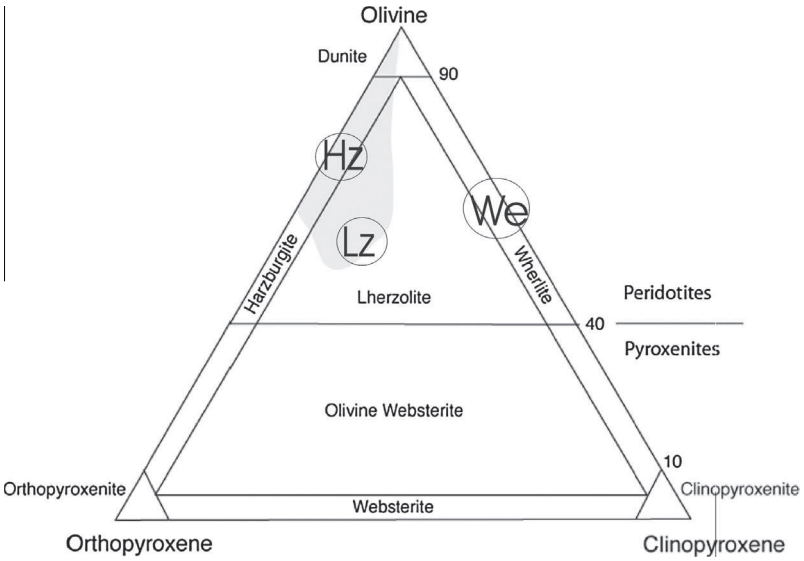

Fig. 2. Ternary diagram showing the mineral proportion of the three types of rocks tested: harzburgite (Hz), lherzolite (Lz) and wehrlite (We) in modal fraction of olivine, orthopyroxene and clinopyroxene. The grey zone corresponds to the average composition of rocks from the Earth's mantle (ophiolite – New Caledonia case – and ultramafic complexes).

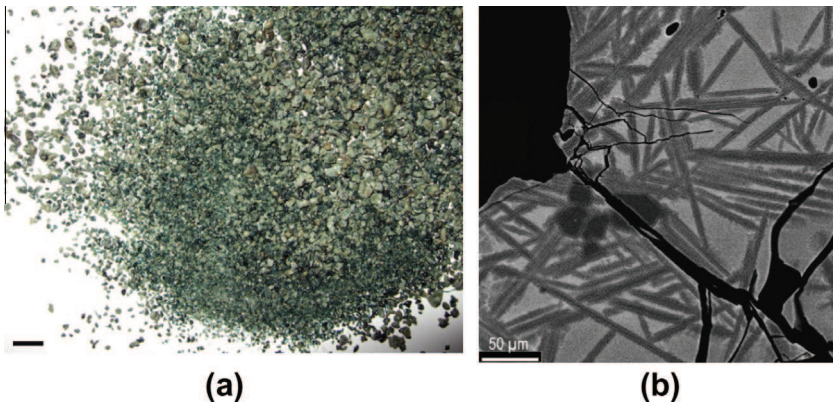

Fig. 3. Fresh pyrometallurgical Ni slag: (a) macroscopic observation (scale bar around 1 cm); (b) SEM image: a tangle of quench dendritic olivine crystals within an amorphous matrix (glass) and larger euhedral olivine crystals. Note the presence of cracks with quenching.

microscope: a vitreous phase and the minor presence of olivine, with internal fractures. Finally a synthetic olivine produced by Magnolithe GmbH was used as a model material during this work (Bonfils, 2012). It is obtained after 1600 °C calcination of natural dunites – serpentinization rate between 40% and70% – coming from an open pit at St Stefan ob Leoben (Austria).

3.2. Rock and slag chemical and mineralogical composition

3.2.1. Methods

Representative aliquots of the dried materials were crushed (<80 µm). The major elements were determined by X-ray fluorescence (Philips PW2400, sequential) following alkaline fusion at 1000 °C using the bead technique by adding lithium tetraborate fluxing agent and then by HCl digestion. Total carbon (Total C) were determined by Lecco method (non-dispersive infrared analysis of the CO_2 gas after treatment). Using the same method, some inorganic carbon analyses (not given hereafter) were also performed to confirm the data and the absence of organic pollution. Fe(II) measurement was performed by titration (bichromate) after mild acid leach of slag (H_2SO_4/HF).

X-ray diffraction (XRD) patterns were recorded on unoriented powder samples using a Siemens D5000 diffractometer with a monochromator, Bragg–Brentano geometry, and Co Ka1 radiation: 4–84°2Θ interval; 1 s/0.02 2Θ step on a rotating sample.

Rock samples and slag were prepared as polished thin sections and examined using optical microscope, scanning electron microscope (SEM, TESCAN) coupled with qualitative energy dispersive spectrometry (SEM/EDS) and minerals were analysed using an electron microprobe (Cameca SX 50) equipped with quantitative wavelength dispersive spectrometer (EMP/WDS). For the latter conditions are: acceleration voltage of 15 keV, reference current of 12 nA, counting time 20 s. The standards used are: albite for Si Ka and Na Ka, orthose for K Ka, wollastonite for Ca Ka, Fe_2O_3 for Fe Ka, MgO for Mg Ka, Al_2O_3 for Al Ka, Cr_2O_3 for Cr Ka, NiO for Ni Ka, $MnTiO_3$ for Ti Ka and Mn Ka. Matrix effect corrections were made with the "PAP" program (Pouchou and Pichoir, 1991).

3.2.2. Composition

Global chemical analyses expressed as oxides show that the selected rocks are rich in Mg and contain some Ca (Table 2). Slags

Table 2
Petrographic data and chemical composition of the samples.

	Hz1	Hz2	We1	Lz1	Slag	Olivine/Magnolithe
Petrographic data						
	Serpentine ≫ olivine > orthopyroxene		Serpentine ≫ olivine > clinopyroxene	Serpentine > olivine > clino/ orthopyroxene	Vitreous fraction ≫ olivine	Olivine > orthopyroxene
Chemical composition (majors %)						
Al_2O_3	0.6	1.3	3.7	4,0	2.5	0.23
CaO	**0.6**	**0.9**	**4.9**	**5.0**	**0.2**	**0.17**
Fe_2O_3tot.	7.8	7.3	7.5	7.6	12,0	9.79
K_2O	<0.05	<0.05	<0.05	<0.05	0.07	0.01
MgO	**41.1**	**40.4**	**32**	**30.8**	**31.9**	**47.35**
MnO	0.12	0.1	0.14	0.15	0.53	0.14
Na_2O	<0.2	<0.2	<0.2	<0.2	<0.2	0.05
P_2O_5	<0.05	<0.05	<0.05	<0.05	<0.05	0.04
SiO_2	40	39.3	44.6	46.3	52.6	41.78
TiO_2	<0.05	<0.05	<0.05	<0.05	0.05	0.01
LOI (1000 °C)	**9.12**	**10.36**	**6.17**	**5.67**	**<0.1**	**<0.1**
Total	99.34	99.66	99.01	99.52	99.85	99.57
Total C (initial)	0.11	0.1	<0.1	0.12	0.13	0.04
Fe(II)O	nm	nm	nm	nm	10.94	nm
Traces (mg/kg DM)						
Cr	2809	2026	3422	1256	6561	nm
Ni	2450	2319	1075	1663	710	nm

nm: non-measured; LOI: lost on ignition; Figures in bold can influence carbonation rates.

also contain potentially carbonable Fe(II). Like most peridotite from New Caledonia, Hz1 and Hz2 contain about 88% serpentine (determined by optical microscope image analysis and in agreement with LOI 9.1–10.4%), 10% olivine and rare occurrence of Mg, Fe pyroxenes – enstatite type. Average structural formulae of olivine determined by microprobe is [$(Mg_{1.83},Fe_{0.07})SiO_4$]. Wehrlite and lherzolite are also composed of serpentinized olivine but to a lesser extent (LOI 5.6–6.2%). They also contain Ca, Mg, Fe pyroxenes – diopside and augite type. The analytical conditions (XRD) are insufficient to characterise the nature of serpentine (lizardite, chrysotile, antigorite – three different monoclinic but with crystallographic settings minerals) with general formula $Mg_3(Si_2O_5)(OH)_4$. Chrysotile (asbestos) is the most common form; however, literature data (Pelletier, 2003) indicate that the primary serpentine in peridotites not affected by supergene alteration is lizardite. Slags are composed of a silico-magnesian amorphous phase, referred as glass hereafter, of composition similar to the global composition and of olivine/forsterite crystals. Quench dentritic olivine and larger euhedral olivine $(Mg_{1.90},Fe_{0.1})SiO_4$ represent about 30% of the slag. Olivine Magnolithe composition varies between $(Mg_{1.88}Fe_{0.12})SiO_4$ and $(Mg_{1.82},Fe_{0.18})SiO_4$.

3.2.3. Preparation, particle size distribution

Before carbonation tests, all solids were ground below 200 μm, 100 μm and even 20 μm – from several kgs prepared at the beginning of the project. Harzburgite (Hz2) was also treated at 550 °C and 650 °C in an oven during 2 h to partly deshydroxylate serpentine into olivine – as confirmed by XRD. Laser diffraction particle size analyses were performed using a Malvern Mastersize apparatus. Typical Hz2 < 100 μm data are: d_{50} = 20 μm; d_{90} = 80 μm; d_{32} in the 4.1–4.7 μm range (surface area mean Sauter diameter) with no significant change with heat treatment neither with carbonation. Slag data <20 μm are: d_{50} = 5 μm; d_{90} = 17 μm; d_{32} = 2.3 μm.

3.3. Experimental set-up and methodology

Direct (i.e. one step) aqueous carbonation tests were performed on ground samples. Process parameters of interest were operating $P(CO_2)$ and T°, Solid/Liquid ratio, and use of organic (mainly oxalates) and inorganic additives (NaCl, $NaCl/NaHCO_3$). Contrarily to organic polyacids which weaken the Mg-O bounds within the mineral structure to promote dissolution, the inorganic salts are believed to mainly act in solution to increase carbonation step. Addition of $NaHCO_3$ reduces the concentration of Mg^{2+} required to precipitate magnesite, promoting carbonation reaction (Chen et al., 2006). NaCl improves the solubility of magnesium silicate (Chen et al., 2006) and also affects the formation of the silica passivating layer (Gorrepati et al., 2010; Wang and Giammar, 2013).

Throughout this project, it was found repeatedly that understanding the performance of such a complex geochemical system requires systematic and comprehensive analysis of both liquid and solid phases. Such analytical work is time and energy intensive, but investigation of one phase only, the liquid phase being simplest, is insufficient and possibly misleading for sound analysis of aqueous mineral carbonation systems. Thus, the experimental work was completed by detailed chemical analysis of water and solid phases and thermodynamic geochemical modelling (using Chess http://chess.geosciences.ensmp.fr/ and PhreeqC v2.18 with the Thermoddem thermodynamic database http://thermoddem.brgm.fr/ (Blanc et al., 2012). In addition, fine mineralogical characterisation of reaction products was carried out using SEM, XRD, laser diffraction particle size analysis and TEM imaging of nanothin section prepared by FIB technique (details in Bonfils et al., 2012). Local analysis of reaction products provided valuable information about the conditions of formation of passivation layers and the nature of reaction by-products.

3.3.1. Set-ups

Two distinct test benches were used during this work, which differ in volume and range of possible operating conditions.

Set-up 1: The equipment is composed of a 2 L stirred autoclave reactor with a Teflon inner jacket equipped with a magnetic stirrer that can maintain a rotating speed as high as 1500 rpm, is rated up to 200 bar and 343 °C. Starting with a standard liquid CO_2 bottle, the CO_2 is compressed via a mechanical pressure booster to 200 bar. The whole compression system is assembled inside a dedicated closet that is kept at a temperature about 45 °C, so that CO_2 remains supercritical in the system that feeds the autoclave. The control panel controls the operating total pressure inside the autoclave chamber via an electromagnetic CO_2 injection valve and the temperature via a heating coil.

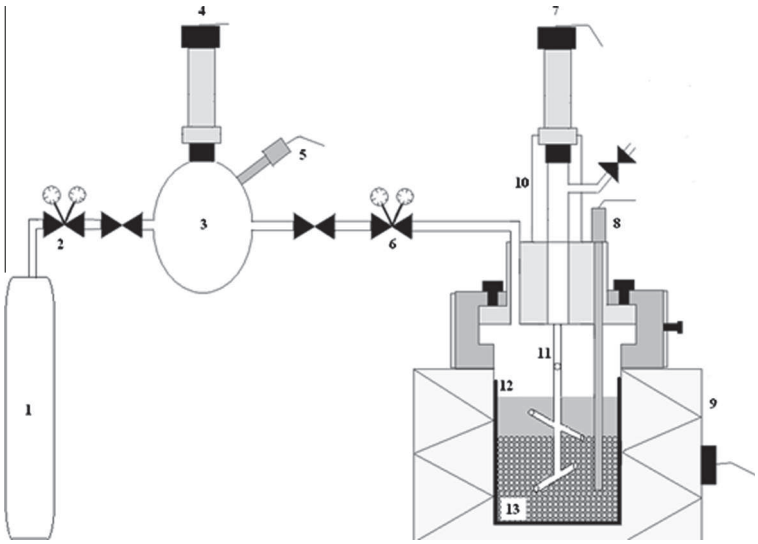

Fig. 4. Schematic diagrams of the attrition autoclave reactor. 1 CO_2 bottle, 2 pressure regulation valve, 3 gas reservoir, 4 pressure transducer, 5 Pt-100 probe, 6 pressure regulation valve, 7 pressure transducer, 8 Pt-100 probe, 9 furnace, 10 magnetic drive, 11 attrition/gas dispersion stirrer, 12 glass inner jacket, 13 grinding media.

Set-up 2: The experimental set-up comprises a 300 mL stirred autoclave reactor with a glass inner jacket and Hastelloy internals. The CO_2 pressure inside the reactor is regulated using a CO_2 ballast tank, and instantaneous CO_2 consumption by the liquid–solid suspension is monitored by recording temperature and pressure inside the ballast. The slurry is stirred by a gas inducing stirrer that achieves high gas–liquid mass transfer. Slurry temperature is monitored and PID controlled (more details in Bonfils et al., 2012). Also, this set-up has been adapted for the experiment described in Section 4.3: the attrition stirrer consists in hollow shaft with arms that also efficiently disperses the gas into the slurry (Fig. 4). The instantaneous CO_2 consumption by the liquid–solid suspension was monitored by application of Peng–Robinson state equation to temperature and pressure signals measured inside a CO_2 ballast feeding the reactor at constant pressure. The difficulty is that the recorded pressure drop also incorporates the reactor headspace filling stage and CO_2 dissolution stage that could be concomitant with carbonation, especially with finely grinded material. Therefore the carbonation yield at the end of the reaction was independently evaluated from both carbon content and thermogravimetry analyses of the final and initial materials. These analyses showed deviations of less than 10% in most cases.

3.3.2. Water analyses and material characterisation

Set-up 1: After filtration at 0.2 μm, pH and alkalinity was measured. Major anions and cations were analysed by ICP-OES and chromatography (IC). Solid were dried and characterised as described above for initial solids (total carbon analyses, XRD, SEM). *Set-up 2:* After filtration using a 0.2 μm micropore filter liquid phase was analysed by ICP-AES to determine the amount of dissolved minerals (Mg, Fe, Si). Solid phase was characterised by different techniques: thermogravimetry coupled with infra-red detection of released gases to confirm the amount of carbonates, electronic microscopy (SEM and transmission: TEM) coupled with elemental analysis (EDX) to identify the different mineral phases, and laser diffraction particle size analysis.

3.3.3. Extent of carbonation

The extent of carbonation (or initial Mg converted) is defined as the fraction of Mg from the initial solid that leaches out and precipitates as $MgCO_3$. $MgCO_3$ has been: (1) calculated as a first estimation of carbonation potential of a panel of materials and conditions on preliminary tests; it has been calculated from total carbon after $MgCO_3$ precipitation was confirmed by XRD and/or microscopic observations; and (2) precisely quantified thanks to thermogravimetry analysis (TGA) coupled with infra-red detection of released gases: carbonates formed during reaction were quantified from the TGA weight loss in the temperature range 300–600 °C, corresponding to CO_2 release from the processed material.

3.4. Environmental assessment

Solutions for the capture and storage of CO_2 are all causing additional energy consumptions and generate potential impacts on the environment. To validate the relevance of new solutions for capture and storage, it is necessary to ensure that the benefits due to the reduction of CO_2 emissions offset the overall environmental impacts of the process. Thus, in order to assess the environmental performance of the ex situ mineral carbonation processes studied within the Carmex project, a life cycle assessment (LCA) was performed. The LCA methodology described in ISO 14040 to 14044 (2006) consists in carrying out exhaustive assessment of natural resources and energy consumptions as well as emissions into the environment for every step of the whole process. Three scenarios were defined and compared, using a coal power plant as the source of CO_2 emissions:

Scenario 1: coal power plant without CO_2 capture (reference).
Scenario 2: coal power plant with CO_2 capture and geological storage.
Scenario 3: coal power plant with CO_2 capture and ex situ mineral carbonation.

Concerning coal power plant, CO_2 capture and CO_2 geological storage, the scenarios considered were based on mature and under development technologies. For instance, the technology considered for CO_2 capture is post-combustion capture with monoethanolamine. Also monitoring of geological storage was not considered because of difficult access to data. Possible end-using of carbonation products was not considered at that stage even if application may exist that could reduce global environmental impact. Concerning ex situ mineral carbonation, the scenario considered was based on experimental results obtained within the Carmex project. Within this scenario, different processes tested on the material olivine

were studied: direct aqueous carbonation, direct aqueous carbonation with organic ligands and direct aqueous carbonation with mechanical exfoliation.

The functional unit chosen for the environmental impact assessment was "To produce 1 MW h of electricity with a coal power plant". This unit allows quantifying the service provided by a coal power plant and to compare the different scenarios on a similar basis. The environmental impacts were assessed by means of five indicators selected among the most commonly used indicators in LCA: natural resources depletion, non-renewable primary energy consumption, climate change, terrestrial acidification and photochemical oxidation. These indicators were calculated for the different steps of the process: coal power plant with or without CO_2 capture, CO_2 transport and CO_2 storage.

4. Results

4.1. Direct aqueous carbonation of rocks and slags (set-up 1)

Aqueous carbonation tests (Tables 3 and 4) were performed on the different rocks and slag samples at constant pulp concentration (90 g/L) and temperature (180 °C), mainly at low pressure (10–20 bar CO_2) from 24 to 96 h, in agreement with the operating conditions investigated by Bonfils (2012). Also, tests were performed with addition of NaCl (sea water equivalent salinity: 0.7 M); and tests with NaCl/$NaHCO_3$ considering the same total ionic strength of 0.7 M with concentrations (0.43 M/0.27 M) adapted from Gerdemann et al. (2007) – same molar ratio.

Total carbon analyses and calculated $MgCO_3$ results show significantly different reactivities for rocks (Table 3). The harzburgite – even the most serpentinised – yielded a conversion higher than that for wehrlite and lherzolite, lherzolite having a coarser size distribution than the former – <200 μm against 100 μm. Depending on the experimental conditions Mg carbonates precipitated as 3D microspherules or geometrical shapes (Fig. 5). Serpentine should not react at such temperature since a heat of activation is needed (Gerdemann et al., 2007); in addition geochemical modelling indicates that aqueous solution is surpersaturated with respect to lizardite, i.e. the mineral cannot dissolve – Tremosa and Lassin, personal comm., 2012. The degree of serpentinisation of rocks appears not to be the only criterion to influence reactivity. Other mineralogical composition differences such as the nature of pyroxene can be mentioned as recently stated by Stockmann (2012): orthorhombic magnesian pyroxene – orthopyroxene – being easier to carbonate than monoclinic calco-ferro-magnesian pyroxene – clinopyroxene. Also the different forsterite molar proportion in olivine in the different types of rocks studied could be another hypothesis to explain the differences of reactivities. Molar proportion calculated as Mg/Mg + Fe = XMg give an: average XMg for harzburgite between 91.36 (91.32–92.02), 89.93 for lherzolite (89.16–90.81), and 89.05 for wehrlite (88.93–89.31). A working pressure around 10–20 bar CO_2 (against 150 bar) appears sufficient for the carbonation process, but reaction rates are too low for developing any viable process, considering also that grinding below 100 μm is already an energy intensive process.

Ni slags carbonate readily in water (Table 4), but slag reactivity is greatly improved by the addition of NaCl – in probable relation with the inhibition of the formation of a silica-rich surface as stated by Wang and Giammar (2013) on forsterite – and NaCl/$NaHCO_3$, by increased operating pressure (90 bar CO_2) and also by grinding to <20 μm to increase the surface accessible for carbonation as previously described for numerous other materials. SEM pictures of slag alteration and $MgCO_3$ formation are given as examples (Fig. 6). A proto-serpentine-like phase can also be formed as shown by microscopy and also on XRD diffractograms. Further experiments are still needed to confirm these very encouraging preliminary results.

4.2. Influence of organic ligands (set-up 2)

The value of direct aqueous mineral carbonation in the presence of organic ligands was thoroughly investigated (Bonfils et al., 2012) using olivine (Magnolithe GmbH) and harzburgite Hz1 ground to minus 100 μm. While confirming that this additive-based solution to ex situ mineral carbonation was efficient for mineral dissolution, it was shown to be a dead-end option which could not lead to

Table 3
One step aqueous carbonation tests on rocks (L/S 90 g/L, 180 °C).

Sample	Size dist.	Ref	Media	P(CO_2)	*t* (h)	Final inorg C (%)	Calc. $MgCO_3$ (%)	Calc. initial Mg converted (%)
Hz2	<100 μm	Test V	dem.w.[a]	10	10	0.41	2.88	2.58
		Test I	milliQ	10	24	0.57	4.00	3.91
		Test R	dem.w.	**20**	24	0.69	4.85	4.90
		Test E	milliQ	10	55	0.66	4.64	4.66
		Test H	dem.w.	10	96	0.84	5.90	6.15
Hz2 650 °C	<100 μm	Test U	dem.w.	10	24	1.39	9.76	**9.58**
We1	<100 μm	Test B	dem.w.	10	96	0.07	0.49	0.73
Lz1	<200 μm	Test C	dem.w.	10	96	0.15	1.05	0.31

[a] dem. w.: demineralized water. Figures in bold can influence carbonation rates.

Table 4
Selective one step aqueous carbonation tests on Ni-pyrometallurgical slag (L/S 90 g/L, 180 °C).

Sample	Size distribution	Ref	Media	P(CO_2)	*t* (h)	Final inorg. C (%)	Calc. $MgCO_3$ (%)	Calc. initial Mg converted (%)
Slag	<100 μm	Test J	dem.w.[a]	10	24	0.02	0.14	–
		Test N	dem.w.	**90**	24	0.31	2.18	3.26
		Test K	NaCl 0.7 M	10	24	0.16	1.12	1.68
		Test L	NaCl/$NaHCO_3$[b]	10	24	0.85	5.97	**8.95**
Slag	<20 μm	Test T	dem.w.	10	24	0.07	0.49	–
		Test S	NaCl/$NaHCO_3$[b]	10	24	2.33	16.37	**23.09**

Figures in bold can influence carbonation rates.
[a] dem. w.: demineralized water.
[b] 0.43 M NaCl/0.27 M $NaHCO_3$: sea water ionic strength; adapted from Gerdemann et al. (2007).

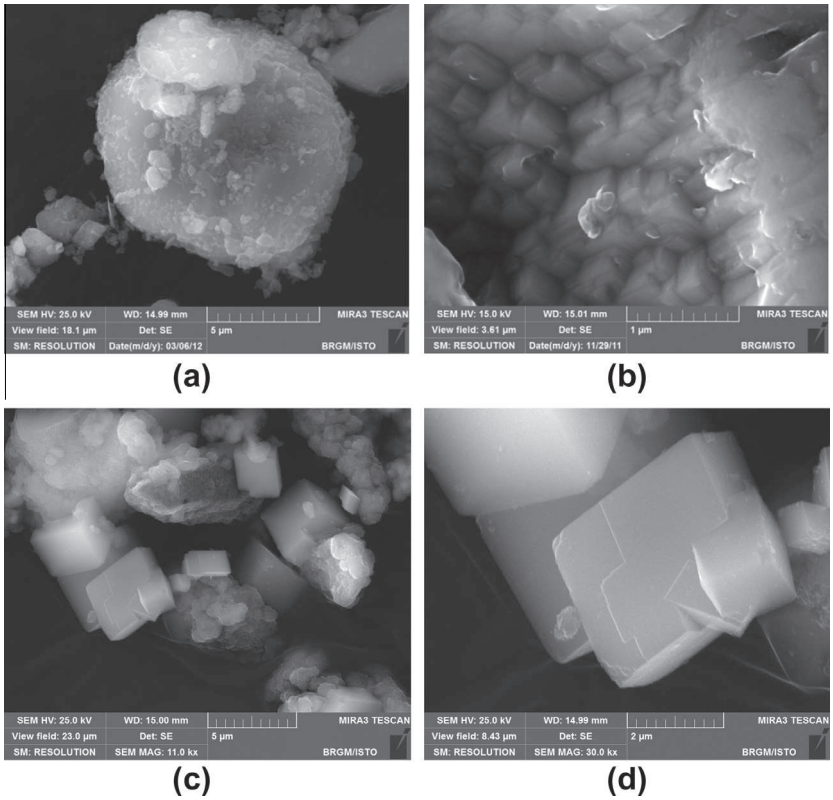

Fig. 5. SEM photographs of carbonation products of harzgurgite: (a) 3D Mg-carbonate microspherule with (b) inside detail (180 °C, 10b CO_2, 96 h, 90 g/L); and of 650 °C calcinated harzurgite: (c) neoformed carbonates with (d) detail (180 °C, 10b CO_2, 24 h, 90 g/L).

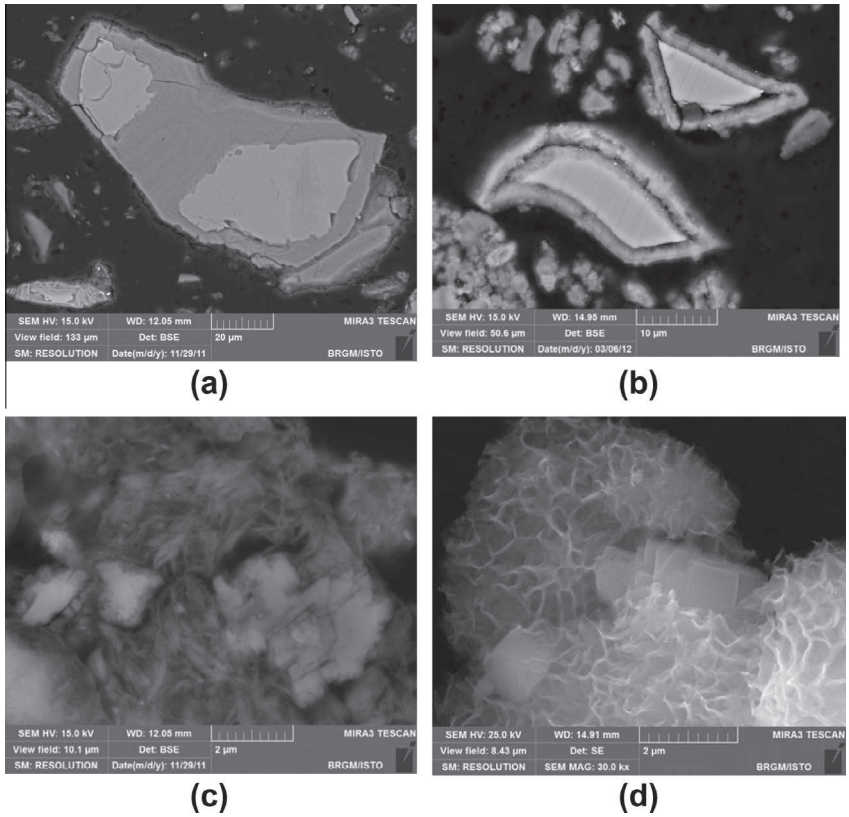

Fig. 6. SEM photographs of carbonation products of Ni slags at 180 °C, 10b CO_2 in water: (a) altered and non-altered glass, (b) altered crust around glass (poor agitation), (c) Mg carbonates in protoserpentine, (d) same in 0.43 M NaCl + 0.27 M $NaHCO_3$.

formation of carbonates (Bonfils, 2012; Bonfils et al., 2012). This work showed that the Mg that would be leached out of the minerals invariably ended up forming a strong complex with the organic component of the additives, in solution and/or in solid form. Glushinskite – $Mg(C_2O_4)\cdot 2(H_2O)$ – for example precipitated in the case of the oxalate additive, preventing any carbonate formation. However, this thorough piece of research led to a number of positive outcomes. It demonstrated that sound research about such complex geochemical systems demands that all phases be analysed simultaneously using a number of complementary analytical techniques, and that the findings to be systematically analysed via appropriate geochemical models and thermodynamic databases. By the same token, detailed analysis of such complex systems highlighted gaps in current thermodynamic databases in relation with elementary reactions, for which data at times exist at ambient temperature only. This situation justifies measurement campaigns of elementary thermodynamic data relevant to mineral carbonation reactions in water.

4.3. Promising development for direct aqueous carbonation of rocks (set-up 2)

Analysis of the carbonation process in water only, without additives, was studied experimentally so as to build additional knowledge on the passivation mechanisms that inhibit dissolution of the magnesium-bearing rocks selected in water. Fig. 7 shows TEM cross-sections of olivine particles having been exposed to 20 bar of CO_2 at 120 °C and 180 °C.

A passivation layer was observed systematically, regardless of material type or test conditions in water. Nevertheless, the nature of the passivation layer showed strong variations in mineralogy, although mainly made of silica, from very thin impervious layers to coarser and more permeable ones. The passivation layers observed at 120 °C and 180 °C differ both from their chemical composition and morphological aspects. A few nanometer thick layer – deemed particularly impervious to fluid transfer – is formed at 120 °C which consists in a mixture of amorphous silica and iron oxide (shown by TEM/EDX analysis), while at 180 °C a phyllosilicate fibrous coating – of less compact appearance – is observed with elemental atomic composition as follows: Mg: 6.26/Si: 8.60/Fe: 0.50. It should be noted that this proto-serpentine is able to encompass excess silicon but does not prevent the formation of magnesium carbonate. This variation in nature indicates that the passivation layer corresponds to the precipitation of silica from the material right after it was leached. Regardless of the type of passivation layer formed around reacting particles, the extent of carbonation never exceeded 7% in 24 h with the rocks tested. The thought process naturally led to considering possibilities for either preventing the formation of the passivation layer, or removing it as it is forming. The lower curve in Fig. 8 shows a typical carbonation rate obtained at 180 °C for olivine particles, with a CO_2 pressure of 20 bars. The dotted line indicates the rate and extent of carbonation that could be obtained if one were able to prevent the formation of the passivation layer on the particle surface. This was estimated through geochemical modelling of the whole system applied to the olivine feed size distribution, using the dissolution rate of the fresh unpassivated surface of the minerals (from Prigiobbe and Mazzotti, 2011); they give the specific dissolution rate in an organic free solution as follows:

$$r = A a_{H+}^{n} e^{\frac{-E_a}{RT}}$$

with A = 2640 mol m^{-2} s^{-1}, n = 0.52 and E_a = 52.9 kJ mol^{-1}.

It has been implemented in the geochemical modelling package CHESS which calculates at each time step the equilibria in solid and liquid phases. Therefore pH and saturation variations have been indeed accounted for. The proposed model also describes the initial particle size distribution, as well as the evolution of the reaction surface according to a shrinking core process.

Faced with the seemingly inevitability of passivation layer formation, the research team investigated the idea of preventing it, as a driving-concept for crossing the gap between the two curves from Fig. 8. Chemical approaches, using catechol for example for selective dissolution of silica, was considered as a possible means for preventing the reprecipitation of silica on the surface of particles during leaching. However, considering that a large scale process is the final target, and factoring potentially significant variations in material type, process conditions, and the possible consumption of chemical additives, a chemically driven solution for preventing the formation of a passivation layer was discarded outright as a potentially non-robust solution. The work was oriented towards prevention of the passivation layer by mechanical means instead. Following the earlier work of Béarat et al. (2006), a dedicated reactor was commissioned at the laboratory scale which would exfoliate the passivation layers mechanically as they would form. Remarkable results were obtained, without optimisation of the process conditions, thereby leaving a significant margin for improvement, both in terms of energy requirement of the overall process and kinetics. The results (Fig. 9) were obtained with minus 100 μm feed particles for five distinct rock samples, without any heat pre-treatment. It is emphasised that some of the rocks exhibit a high degree of serpentinisation, and this seemed to make no difference on the performance, confirming the robustness of mechanical passivation layer in the context of highly variable

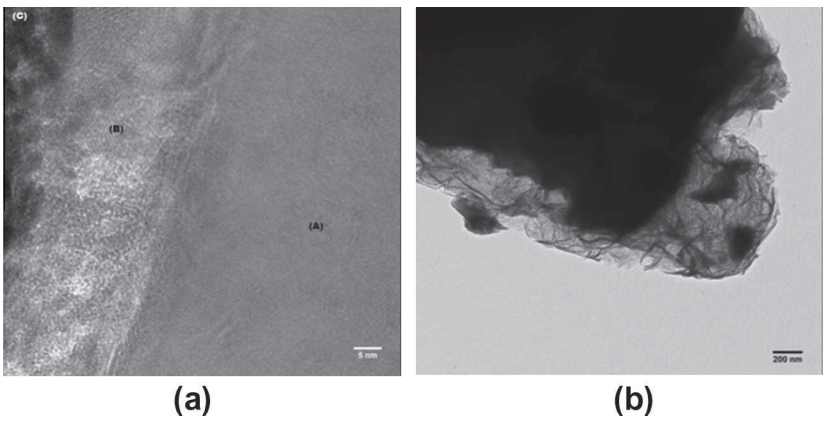

Fig. 7. Visuals of the passivation layers that precipitate around the olivine particles during aqueous mineral carbonation reaction in water only – TEM pictures after reaction at (a) 120 °C (3 g/L, PCO_2 = 20 bar, 24 h reaction time) and (b) at 180 °C (90 g/L, PCO_2 = 20 bar, 95 h reaction time).

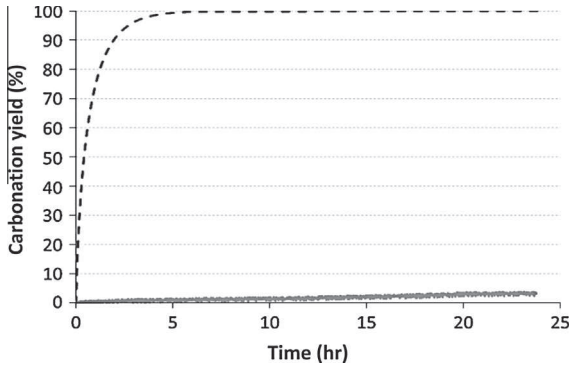

Fig. 8. Extent of carbonation for olivine as a function of time (180 °C, PCO_2 = 20 bar, 90 g/L). The solid line shows a typical measurement for a magnesium silicate ore (minus 100 μm), whereas the dotted line shows the theoretical kinetics expected without passivation.

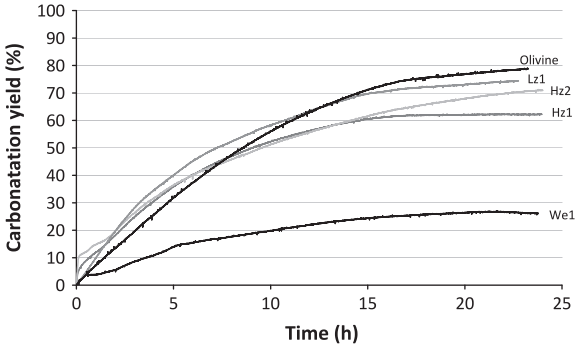

Fig. 9. Kinetics of carbonation as a function of time (180 °C, PCO_2 = 20 bar, 90 g/L) obtained with 5 magnesium silicates with a continuous passivation layer exfoliation scheme.

feed ore properties. Note that the initial rates were obtained by extrapolating the measured dissolution kinetics back to $t = 0$; using the final carbonation yield measured from C content as reference, the CO_2 consumption curve could be backtracked all the way to the very start of the process. It was finally checked that this starting point matched with the time where pressure became steady inside the reactor.

Mechanical exfoliation led to the product being entirely made of very fine magnesite particles and fine remaining cores of unleached material. It was not possible in the experiments to identify

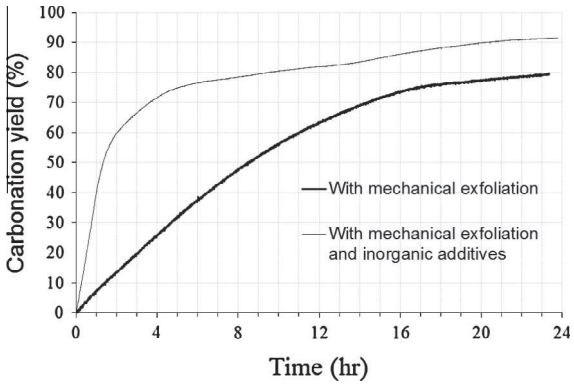

Fig. 11. Acceleration of the mechanical exfoliation carbonation of olivine (90 g/L, 180 °C) using inorganic additives (as proposed by Gerdemann et al. (2007)).

any of the passivation layers that were measured previously (see Fig. 7), proving that the mechanical exfoliation process was successful. SEM and TEM photographs of the product are shown in Fig. 10.

Fig. 10a shows the product, which has a d_{50} of 4 μm, and a top size of slightly over 20 μm. Zooming further on the product particles, Fig. 10b shows that particles are composed of aggregated nanosized magnesite grains, whose geometrical shape is easily recognisable. The fineness of the product was thought to yield difficulties with the recycling of process water, however these were shown to be unfounded as preliminary tests with a laboratory centrifuge operating at 200g yielded an easily dewatered filtration cake. With the product being so fine, it is unlikely that magnesite particles can be separated. Nevertheless, considerations have been given to the beneficiation of the fine reaction product, and preliminary considerations indicate that their properties may be suitable for making magnesium-based cements.

As indicated earlier, optimisation of this process is yet to be carried out, along with a better understanding of the mechanical exfoliation process itself. Thus far, a few variations of this process have been tested, including the addition of the standard 1 M NaCl + 0.64 M $NaHCO_3$ inorganic solution (Gerdemann et al., 2007). This has helped reach carbonation rates in excess of 90% in less than 24 h, as shown in Fig. 11. It is noted that the effect of such additives is strongest initially, with the material reaching 70% conversion in 4 h.

Continuous mechanical exfoliation of passivation layers is deemed to open promising avenues for the development of ex situ mineral carbonation, and is the current focus of a new research project that seeks out industrial feasibility and demonstration.

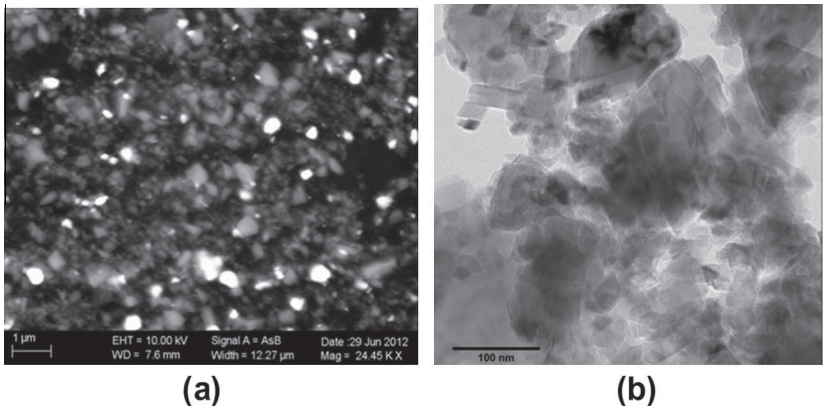

Fig. 10. Reaction product after continuous mechanical exfoliation of passivation layers during the aqueous mineral carbonation reaction: (a) SEM image, (b) TEM image.

Table 5
LCA results for some scenario studied (functional unit: To produce 1 MW h of electricity with a coal power plant).

Environmental impact indicators	Units	Scenario 1: without CO_2 capture	Scenario 2: with CO_2 capture and geological storage	Scenario 3: with CO_2 capture and ex situ mineral carbonation[a]
Natural resources depletion	kg Sb eq.[b]	6.70E+00	9.81E+00	1.20E+01
Non-renewable primary energy consumption	primary MJ	9.99E+03	1.47E+04	2.09E+04
Climate change	kg CO_2 eq.	9.23E+02	2.98E+02	6.08E+02
Terrestrial acidification	kg SO_2 eq.	1.64E+00	1.22E+00	2.50E+00
Photochemical oxidation	kg NMVOC eq.#	9.73E−01	1.34E+00	1.98E+00

[a] Best results obtained: direct aqueous carbonation with mechanical exfoliation.
[b] kg Sb eq. = kg antimony equivalent, antimony using as the resource reference; #NMVOC = Non-Methane Volatile Organic Compounds.

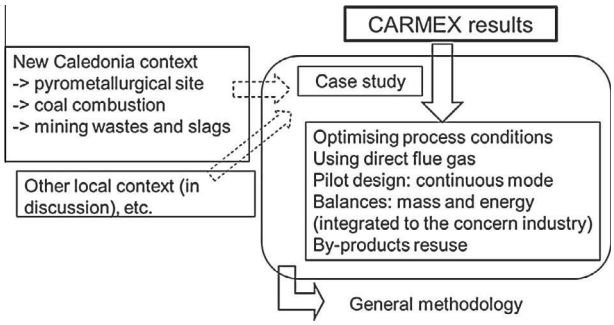

Fig. 12. Perspectives of the project.

5. LCA of aqueous mineral carbonation – Discussion

The LCA carried out allowed quantifying the environmental impacts of the whole process of CO_2 capture and storage for different ex situ mineral carbonation processes tested on olivine: direct aqueous carbonation, direct aqueous carbonation with organic ligands and direct aqueous carbonation with mechanical exfoliation. Moreover, by using the example of a coal power plant as the source of CO_2 emissions, the LCA allowed to compare the environmental impacts of electricity production for three different scenarios: without CO_2 capture, with CO_2 capture and geological storage and with CO_2 capture and ex situ mineral carbonation.

The LCA results (Table 5) highlight the fact that CO_2 capture and storage processes may lead to environmental benefits but also lead in all cases to environmental damages. Indeed, even when the whole process reaches its goal and allows a reduction of the overall CO_2 balance, the additional energy consumptions required for the process are always at the origin of transfers of pollution and worsen some environmental impacts. For instance, for the scenario with CO_2 capture and geological storage, the indicators "Climate change" (CO_2 balance) and "Terrestrial acidification" are respectively reduced by 68% and 26% in comparison with the scenario without CO_2 capture. However, the three other indicators studied show an increase between 40% and 50%. Concerning the scenario with CO_2 capture and ex situ mineral carbonation, the LCA shows that the environmental performance of the whole process varies greatly depending on the carbonation process studied.

For the direct aqueous carbonation processes without mechanical exfoliation (with or without organic ligands), the results obtained for the indicator "Climate change" are multiplied by a factor ranging between 5 and 20 compared to the scenario without CO_2 capture. Other environmental impacts are also aggravated. Indeed, due to the low conversion of Mg into carbonates (between 3% and 15%), these types of carbonation processes are highly energy intensive. Thus, they do not reach their objective and emit more CO_2 than they make it possible to store. For the direct aqueous carbonation processes with mechanical exfoliation, the deviation from the scenario without CO_2 capture is reduced. Moreover, in the best case studied, the high conversion of Mg into carbonates (79.3%) and the high Solid/Liquid ratio (250 g/L) allows reducing the energy consumptions. Under these conditions, the indicator "Climate change" is reduced by 34% and the process achieves its goal in terms of reduction of greenhouse gas emissions.

Thus, while keeping in mind the limitations of this LCA (lack of data for certain steps of the processes – i.e. monitoring of geological storage–, energy consumptions estimated by means of thermodynamic models...), the results show that the process of carbonation with mechanical exfoliation is the most promising from the environmental point of view. Search for carbonation product applications could furthermore reduce global environment impact.

6. Concluding remarks

This article gave an overview of the main outputs from the French Carmex project (2009–2012). This project reviewed the feasibility of ex situ mineral carbonation in terms of mining wastes resource availability, performance of the aqueous mineral carbonation process and life cycle assessment. Firstly, the project demonstrated the value of GIS for identification and ranking of potential sites. Also the project allows achieving significant conversion rates, combining reactive carbonation with mechanical exfoliation, capable of preventing the formation of passivation layers around the particles. Life cycle assessment of the system as a whole led to the conclusion that the eligibility of ex situ mineral carbonation as a practical solution to CO_2 mitigation depends primarily on the operating conditions of the process. This result indicates that more development work is required to optimise the process; however results obtained during this project suggest that admissible conditions are within reach confirming the fact that ex situ mineral carbonation could be a relevant complementary solution to geological CO_2 storage. The New Caledonian context seems particularly favourable.

Current perspectives (Fig. 12) include: (1) optimisation of the process conditions, in a continuous operating mode which is deemed more favourable; (2) thermodynamic mass and energy balance calculations to evaluate the integration of mineral carbonation to actual nickel concentrators; (3) evaluating the possibilities of using diluted fumes, leading to direct use of flue gases; (4) finding out beneficiation routes for reaction products, possibly taking advantage of their mineralogical composition and fine particle size distribution.

Acknowledgements

This research (Carmex Project No. ANR-08-PCO2-002) was co-funded by the French National Research Agency (ANR – CO_2 Capture and Storage programme) and by Total (thesis funding). Special thanks to P. Galle-Cavalloni (BRGM) for his contribution to the

experimental work, to BRGM's Laboratory Division and F. Maldan for GIS maps. The authors acknowledge three reviewers.

References

Alizadehhesari, K., Golding, S.D., Bhatia, S.K., 2012. Kinetics of the dehydroxylation of serpentine. Energy Fuels 26, 783–790.

Béarat, H., McKelvy, M.J., Chizmeshya, A.V.G., Gormley, D., Nunez, R., Carpenter, R.W., Squires, K., Wolf, G.H., 2006. Carbon sequestration via aqueous olivine mineral carbonation: role of passivating layer formation. Environ. Sci. Technol. 40, 4802–4808.

Blanc, P., Lassin, A., Piantone, P., Azaroual, M., Jacquemet, N., Fabbri, A., Gaucher, E.C., 2012. Thermoddem: a geochemical database focused on low temperature water/rock interactions and waste materials. Appl. Geochem. 27, 2107–2116.

Bonfils, B., 2012. Mécanismes et verrous de la carbonatation minérale du CO_2 en voie aqueuse, thèse de Doctorat de l'Université de Toulouse, France (in French). <http://ethesis.inp-toulouse.fr/archive/00002101/>.

Bonfils, B., Julcour-Lebigue, C., Guyot, F., Bodénan, F., Chiquet, P., Bourgeois, F., 2012. Comprehensive analysis of direct aqueous mineral carbonation using dissolution enhancing organic additives. Int. J. Greenhouse Gas Control 9, 334–346.

Chen, Z.Y., O'Connor, W.K., Gerdemann, S.J., 2006. Chemistry of aqueous mineral carbonation for carbon sequestration and explanation of experimental results. Environ. Prog. 25, 161–166.

Doucet, F.J., 2011. Scoping Study on CO_2 Mineralization Technologies. Report No CGS-2011-007. South African Centre for Carbon Capture and Storage.

Foucault, A., Raoult, J.F., 2005. Dictionnaire de la géologie, 6ème édition, Dunod (ed.), Paris. ISBN: 2100490710.

Garcia, B., Beaumont, V., Perfetti, E., Blanchet, D., Oger, P., Dromart, G., Huc, A.-Y., Haeseler, F., 2010. Experiments and geochemical modelling of CO_2 sequestration by olivine: potential, quantification. Appl. Geochem. 25, 1383–1396.

Gerdemann, S.J., O'Connor, W.K., Dahlin, D.C., Penner, L.R., Rush, H., 2007. Ex situ aqueous mineral carbonation. Environ. Sci. Technol. 41, 2587–2593.

Gorrepati, E.A., Wongthahan, P., Raha, S., Fogler, H.S., 2010. Silica precipitation in acidic solutions: mechanism, pH effect, and salt effect. Langmuir 26, 10467–10474.

Guyot, F., Daval, D., Dupraz, S., Martinez, I., Menez, B., Sissmann, O., 2011. CO_2 geological storage: the environmental mineralogy perspective. C.R. Geosci. 343, 246–259.

Hitch, M., Dipple, G.M., 2012. Economic feasibility and sensitivity analysis of integrating industrial-scale mineral carbonation into mining operations. Miner. Eng. 39, 268–275.

Hitch, M., Ballantyne, S.M., Hindle, S.R., 2009. Revaluing mine was rock for carbon capture and storage. Int. J. Min. Reclam. Environ., 1–16.

Huijgen, W.J.J., Comans, R.N.J., 2003. Carbon Dioxide Sequestration by Mineral Carbonation: Literature Review. Energy Research Center of the Netherlands.

Huijgen, W.J.J., Comans, R.N.J., 2004. Carbon Dioxide Sequestration by Mineral Carbonation: Literature Review Update 2003–2004. Energy Research Center of the Netherlands.

Huijgen, W.J.J., Witkamp, G.-J., Comans, R.N.J., 2005. Mineral CO_2 sequestration by steel slag carbonation. Environ. Sci. Technol. 39, 9676–9682.

IEA, 2006. International Energy Agency. Global GHG CO_2 Emissions Database.

IPCC, 2005. Mineral carbonation and industrial uses of carbon dioxide. In: Metz, Bert, Davidson, Ogunlade, de Coninck, Heleen, Loos, Manuela, Meyer, Leo (Eds.), Carbon Dioxide Capture and Storage. Cambridge University Press, UK. pp. 431 (Chapter 7). <http://www.ipcc.ch/pdf/special-reports/srccs/srccs_chapter7.pdf>.

ISO 14040 to 14044, 2006. Standard, Environmental Management – Life Cycle Assessment – Principles and Framework; Requirements and Guidelines.

Krevor, S.C., Lackner, K.S., 2011. Enhancing serpentine dissolution kinetics for mineral carbon dioxide sequestration. Int. J. Greenhouse Gas Control 5, 1073–1080.

McKelvy, M.J., Chizmeshya, A.V.G., Diefencacher, J., Bearat, H., Wolf, G., 2004. Exploration of the role of heat activation in enhancing serpentine carbon sequestration reactions. Environ. Sci. Technol. 38, 6897–6903.

O'Connor, W.K., Dahlin, D.C., Nielsen, D.N., Rush, G.E., Walters, R.P., Turner, P.C., 2001. Carbon Dioxide Sequestration by Direct Mineral Carbonation: Results from Recent Studies and Current Status. Albany Research Center, Albany, Oregon.

O'Connor, W.K., Dahlin, D.C., Rush, G.E., Gerdemann, S.J., Penner, L.R., 2004. Energy and Economic Considerations for ex-situ Aqueous Mineral Carbonation. U.S. Department of Energy, Albany Research Center, Albany, Oregon.

Olsen, A.A., Rimstidt, J.D., 2008. Oxalate-promoted forsterite dissolution at low pH. Geochim. Cosmochim. Acta 72, 1758–1766.

Pelletier, B., 2003. Les minerais de nickel de Nouvelle-Calédonie. Géologue 138, 30–38.

Picot, J.C., Cassard, D., Maldan, F., Greffié, C., Bodénan, F., 2011. Worldwide potential for ex-situ mineral carbonation. Energy Proc. 4, 2971–2977.

Pouchou, J.L., Pichoir, F., 1991. Quantitative analysis of homogeneous or stratified microvolumes applying the model "PAP". In: Heinrich, K.F.J., Newbury, D.E. (Eds.), Electron Probe Quantitation. Plenum Press, New York, pp. 31–75.

Prigiobbe, V., Mazzotti, M., 2011. Dissolution of olivine in the presence of oxalate, citrate, and CO_2 at 90 °C and 120 °C. Chem. Eng. Sci. 66, 6544–6554.

Renforth, P., Washbourne, C.-L., Taylder, J., Manning, D.A.C., 2011. Silicate production and availability for mineral carbonation. Environ. Sci. Technol. 45, 2035–2041.

Rundqvist, D., Cassard, D., Cherkasov, S., Tkachev, A., Vishnevskaya, N., Arbuzova, E., Gateau, C., Husson, Y., 2006. Largest Ore Deposits of the World. NavigasSIG Large and Superlarge Deposits v1.0 CD-ROM, August 2006, Russian-French Metallogenic Laboratory Editor, Moscow. ISBN: 5-9900765-1-7.

Sanna, A., Hall, M.R., Maroto-Valer, M., 2012. Post-processing pathways in carbon capture and storage by mineral carbonation (CCSM) towards the introduction of carbon neutral materials. Energy Environ. Sci. 5, 7781–7796.

Seifritz, W., 1990. CO_2 disposal by means of silicates. Nature 345, 486.

Sipilä, J., Teir, S., Zevenhoven, R., 2008. Carbon Dioxide Sequestration by Mineral Carbonation: Literature Review Update 2005–2007. Abo Akademi University, Heat Engineering Laboratory, Finland.

Stockmann, G.J., 2012. Experimental Study of Basalt Carbonatization. Ph-D Thesis. University Toulouse, France (in English). <http://thesesups.ups-tlse.fr/1572/>.

Stockmann, G.J., Wolff-Boenisch, D., Gislason, S.R., Oelkers, E.H., 2011. Do carbonate precipitates affect dissolution kinetics? 1: basaltic glass. Chem. Geol. 284, 306–316.

Tremosa, J., Lassin, A., 2012. Carbonation of a Natural perdidotite (Harzburgite): Experiments and Numerical Simulations. Carmex Project. Personal comm.

Wang, F., Giammar, D.E., 2013. Forsterite dissolution in saline water at elevated temperature and high CO_2 pressure. Environ. Sci. Technol. 47, 168–173.